



THE UNIVERSITY *of* EDINBURGH

Edinburgh Research Explorer

Time-dependent behaviour of demineralised trabecular bone – experimental investigation and development of a constitutive model

Citation for published version:

Xie, S, Wallace, R & Pankaj, P 2020, 'Time-dependent behaviour of demineralised trabecular bone – experimental investigation and development of a constitutive model', *Journal of the mechanical behavior of biomedical materials*, vol. 109, 103751. <https://doi.org/10.1016/j.jmbbm.2020.103751>

Digital Object Identifier (DOI):

[10.1016/j.jmbbm.2020.103751](https://doi.org/10.1016/j.jmbbm.2020.103751)

Link:

[Link to publication record in Edinburgh Research Explorer](#)

Document Version:

Peer reviewed version

Published In:

Journal of the mechanical behavior of biomedical materials

General rights

Copyright for the publications made accessible via the Edinburgh Research Explorer is retained by the author(s) and / or other copyright owners and it is a condition of accessing these publications that users recognise and abide by the legal requirements associated with these rights.

Take down policy

The University of Edinburgh has made every reasonable effort to ensure that Edinburgh Research Explorer content complies with UK legislation. If you believe that the public display of this file breaches copyright please contact openaccess@ed.ac.uk providing details, and we will remove access to the work immediately and investigate your claim.



Time-dependent behaviour of demineralised trabecular bone – experimental investigation and development of a constitutive model

1 **Shuqiao Xie¹, Robert J. Wallace², Pankaj Pankaj^{1*}**

2 ¹School of Engineering, Institute for Bioengineering, The University of Edinburgh, Alrick Building,
3 The King's Buildings, Edinburgh EH9 3BF, UK

4 ²Department of Orthopaedics, The University of Edinburgh, Chancellor's Building, Edinburgh EH16
5 4SB, UK

6 *** Correspondence:**

7 Professor Pankaj Pankaj

8 pankaj@ed.ac.uk

9

10 **Abstract**

11 Trabecular bone is a cellular composite material comprising primarily of mineral and organic phases
12 and its mechanical response to loads is time-dependent. The contribution of the organic phase to the
13 time-dependent behaviour of bone is not yet understood. We investigated the time-dependent
14 response of demineralised trabecular bone through tensile multiple-load-creep-unload-recovery
15 experiments. We found that demineralised trabecular bone's time-dependent response is nonlinearly
16 related to the applied stress levels - it stiffens with increased stress levels. Our results also indicated
17 that the time-dependent behaviour is associated with the original bone volume ratio (BV/TV).
18 Irrecoverable strain exists, even at the low strain levels, but are not associated with BV/TV.
19 Furthermore, we found that the nonlinear viscoelastic model can accurately predict the time-
20 dependent behaviour of the trabecular bone's organic phase, which can be incorporated together with
21 the properties of mineral to generate a composite model of bone. This study will help to provide a
22 better understanding of this natural composite material.

23

24 **Keywords:** Bone volume ratio, recoverable and irrecoverable strain, nonlinear viscoelasticity,
25 collagen, creep compliance.

26

27 **1 Introduction**

28 Bone has been known to be a composite material which comprises of a mineral phase (mainly
29 carbonated hydroxyapatite), organic phase (mostly type I collagen) and water assembled into a
30 complex, hierarchical structure (Currey 1964). Currey (1969) also described the time-independent
31 mechanical properties of bone (e.g. elastic modulus) as a function of its ash content and showed that
32 it increases with increasing mineralisation. However, since bone is not an isotropic material its
33 mineral density is not the only determinant of its elastic modulus. This was confirmed by Bonfield
34 and Li (1967) who reported a variation in Young's modulus with orientation. Later, a two-level
35 hierarchical fibre-reinforced composite model of bone was developed by Katz (1980) to quantify the
36 effect of orientation. Literature shows that the subject of developing the time-independent elastic
37 properties of bone as a function of its constituents has been a subject of research for the past five
38 decades.

39 The organic phase of bone can be isolated through a demineralisation process, which generally
40 comprises of submerging bone samples in a chemical solution, e.g. ethylenediaminetetraacetic acid
41 (EDTA) or hydrochloric acid (HCl). One of the earliest studies on the mechanical properties of
42 demineralised bone was by Burstein et al. (1975), who examined the tensile mechanical behaviour of
43 progressively demineralised cortical bone obtained from bovine tibia by using HCl solution of
44 varying concentration (0.005-0.5N); the authors showed that the ultimate stress, yield stress and
45 Young's modulus decreased progressively with increasing HCl solution concentration. Other studies
46 on demineralised bone examined its elastic behaviour (Bowman et al. 1996; Catanese et al. 1999;
47 Chen and McKittrick 2011; Novitskaya et al. 2011) and its cyclic behaviour (Novitskaya et al. 2013).
48 A number of studies have shown a nonlinear load-deformation response from monotonic loading
49 experiments (Bowman et al. 1996; Catanese et al. 1999; Novitskaya et al. 2011) and cyclic loading
50 tests (Novitskaya et al. 2013; Xie et al. 2018b). However, studies that have considered time-
51 dependent behaviour of demineralised trabecular bone have been limited (Bowman et al. 1994).

52 It has been widely recognised that the mechanical response of bone, when subjected to loads, is not
53 instantaneous, but is time-dependent (Bowman et al. 1994; Manda et al. 2016, 2017; Xie et al. 2017).
54 However, the contribution of the constituent components of bone to its time-dependent behaviour has
55 received little attention. Bowman et al. (1999) investigated the creep behaviour of fully demineralised
56 cortical bone at varying normalised stresses and reported that the samples possessed three classical
57 regimes of creep – primary, secondary and tertiary. Although this study considered varying load

58 levels, it achieved this by applying different load levels to different samples, i.e. each sample was
59 subjected to a single load level only. By conducting fully reversed cyclic tension-compression loads
60 with varying load on demineralised trabecular bone samples, asymmetric behaviour – stiffening in
61 tension and softening in compression – was observed (Xie et al. 2018b). However, this cyclic
62 experimental protocol could not be used readily for the development of time-dependent constitutive
63 models.

64 In summary, while there have been a number of studies to examine the time-independent behaviour
65 of demineralised bone (Bowman et al. 1999; Catanese et al. 1999; Chen and McKittrick 2011;
66 Novitskaya et al. 2011), studies examining its time-dependent response are lacking (Bowman et al.
67 1996; Xie et al. 2018b). Therefore, the primary objectives of this study were as follows. Firstly, to
68 experimentally evaluate the time-dependent behaviour of demineralised trabecular bone by
69 undertaking creep and recovery experiments at multiple load levels. Secondly, to describe the
70 experimental results using time-dependent constitutive models. Lastly, by performing micro-
71 computed tomography (μ CT) on the samples prior to demineralisation, evaluate how the response is
72 influenced by the original bone volume ratio (BV/TV).

73 **2 Materials and methods**

74 **2.1 Sample preparation**

75 Four fresh bovine proximal tibias under 30 months old when slaughtered were obtained from a local
76 abattoir and stored at -20°C until utilised. The bones were allowed to thaw at room temperature
77 before bone cores were extracted along its principal axis, using diamond coring tools with an inner
78 diameter of 10.7 mm (Starlite, Rosemont, IL, USA). A low speed rotating saw (Buehler, Germany)
79 was used to create parallel sections and to trim growth plates if they were present. All coring and
80 cutting was conducted in a water bath to reduce heat generation. The cylindrical bone samples ($n=7$)
81 had a mean height of 20.4 ± 0.7 mm.

82 Bone marrow was removed from each sample using a dental water jet (Interplak, Conair) with tap
83 water at room temperature (Lievers et al. 2007). All the samples were then centrifuged at 2000 r.p.m
84 for 2 hours to remove any residual marrow (Sharp et al. 1990). All the samples were scanned using
85 μ CT scanner (Skyscan 1172, Bruker, Kontich, Belgium) at a resolution of $17.22 \mu\text{m}$ and the system's
86 software (CTan, v1.13.5.1) was used to evaluate the bone volume to total volume ratio (BV/TV) of
87 the bone, which was found to be in the range 15.5 - 37.6 %. Scanning parameters used were: source

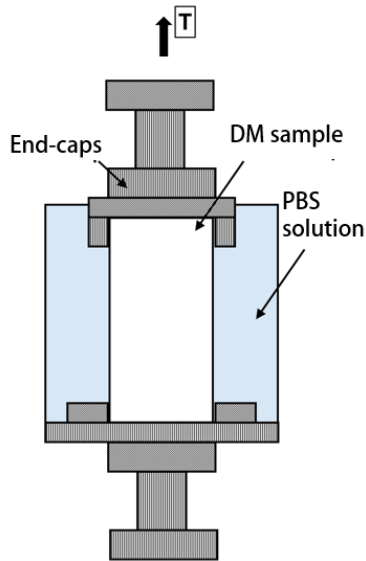
88 voltage 54 kV, current 185 μ A, exposure 885 ms with a 0.5 mm aluminium filter between the X-ray
89 source and the sample. The image quality was improved by using 2 frames averaging. It should be
90 noted that the BV/TV mentioned in this study relates to the bone volume ratio of the sample prior to
91 demineralisation.

92 **2.2 Demineralisation**

93 After scanning, demineralisation was conducted by submerging samples in 20 ml 0.6N hydrochloric
94 acid (HCl) at room temperature. The tubes were loaded into a wire rack to secure and vertically
95 orientate them, before being placed in an ultrasonic tank. Ultrasonic agitation was applied at a
96 frequency of 20kHz in order to increase the rate of demineralisation (Wallace et al. 2013).
97 Hydrochloric acid has been successfully used for demineralising bone in previous studies (Burstein et
98 al. 1975; Chen et al. 2011; Chen and McKittrick 2011; Castro-Ceseña et al. 2013; Xie et al. 2018b).
99 The solution was changed daily (Chen and McKittrick 2011) for two weeks after which the
100 completeness of demineralisation was verified using μ CT scanning. All samples in this study were
101 found to be fully demineralised in 2 weeks.

102 **2.3 Mechanical testing**

103 Samples were fixed into end-caps using bone cement (Simplex, Stryker, UK) with the assistance of a
104 custom made alignment tool in order to minimise the end-artefacts during testing (Keaveny et al.
105 1997). Bone cement had a Young's modulus above 1 GPa which is much higher than the modulus of
106 demineralised bone sample. Therefore, the strain response of bone cement layer can be assumed to be
107 negligible in comparison to that of the sample. The effective length (17.4 ± 0.7 mm) of each sample
108 was calculated as the exposed length of the sample between the end-caps plus half the length of the
109 sample embedded within the end-caps (Keaveny et al. 1997). Each sample was placed in an epoxy
110 tube filled with phosphate-buffered saline (PBS) solution to ensure that they remained hydrated
111 during all stages of mechanical testing (Xie et al. 2018b) as shown in Fig. 1.



112

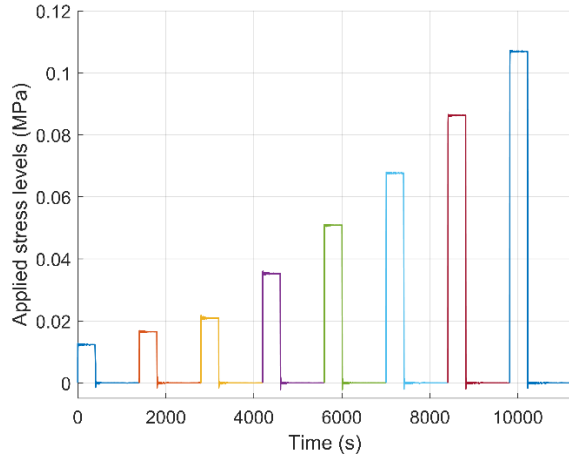
113 *Figure 1: Schematic representation of loading set up. Samples are kept hydrated in a PBS solution throughout*
 114 *mechanical testing*

115 Each sample was first preconditioned by subjecting it to 10 cycles of tensile loading with an
 116 amplitude of 0.1 % apparent strain (Xie et al. 2017). The tensile multiple-load-creep-unload-recovery
 117 (MLCUR) experiment was conducted on 7 fully demineralised trabecular bone samples using Instron
 118 material testing machine (50N load cell, Model 3367) at room temperature. These tests comprised of
 119 cyclic loading in which samples were loaded, permitted to undergo creep, unloaded and then left to
 120 recover.

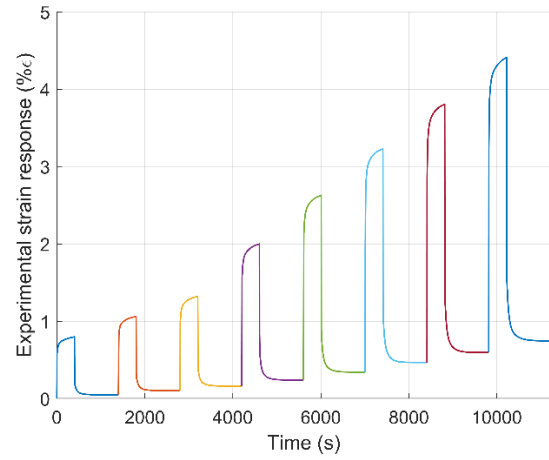
121 Bone has been shown to yield at relatively isotropic strains as compared to stresses, and the yield
 122 strain is not dependent upon apparent elastic stiffness or density (Vahey et al. 1987; Levrero-
 123 Florencio et al. 2016). Consequently strain-based loading cycles were applied. Loading cycles
 124 comprised static loading strain of 0.6 %, 0.8 %, 1.0 %, 1.5 %, 2.0 %, 2.5 %, 3.0 % and 3.5 %
 125 apparent static strains at the rate of 0.01s^{-1} . Loading and unloading phases were under displacement
 126 control. The chosen strain rate has been successfully used previously to characterise the time-
 127 dependent behaviour of trabecular bone (Manda et al. 2016, 2017; Xie et al. 2017). When the
 128 designated target strain was achieved, the corresponding load was maintained for 400 s, thereby
 129 permitting the sample to undergo creep. For a typical sample, (medium porosity, $BV/TV = 26.8\%$)
 130 corresponding load levels are shown in Fig. 2a. Each loading step was followed by an unloading step
 131 to a zero force at the same rate used for loading (0.01 s^{-1}) and this zero force was maintained for
 132 1000s before proceeding to the next cycle (Fig. 2a). These durations for creep and recovery were

133 determined after initial pilot tests which showed that 400 s and 1000 s were more than sufficient for
134 the samples to achieve a constant creep rate and for recovery curves to reach a plateau, respectively.
135 The dataset for these demineralised trabecular bone samples under tensile multiple-load-creep-unload
136 experimental are available from Edinburgh DataShare (Xie et al. 2018a).

137



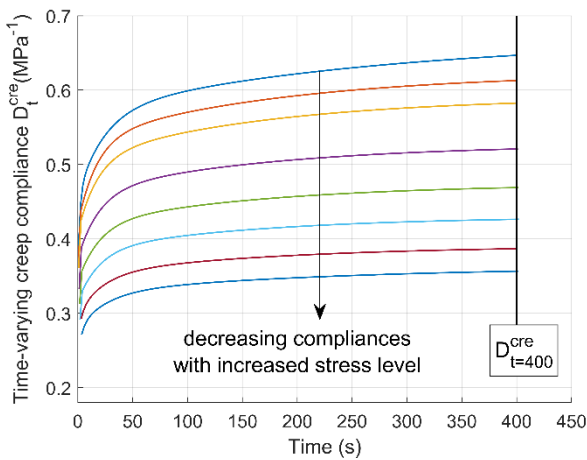
(a)



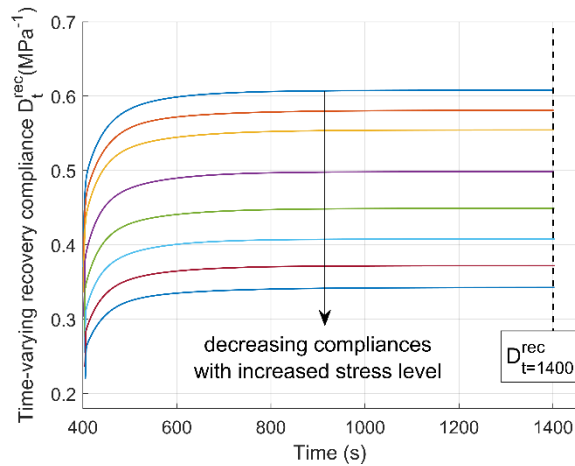
(b)

138

139



(c)



(d)

140

141

142 *Figure 2: Response of a typical sample ($BV/TV = 26.8\%$) subjected to tensile multiple-load-creep-unload-*
 143 *recovery cycles. Load application (a); strain response (b); time-varying creep compliance (c) and recovery*
 144 *compliance (d) at varying stress levels. In each cycle, plateau load was held constant for 400 s and strain*
 145 *recovery was measured for another 1000s before next cycle application. The applied load in each cycle*
 146 *corresponds to the static strain of 0.6 %, 0.8 %, 1.0 %, 1.5 %, 2.0 %, 2.5 %, 3.0 % and 3.5 %*

147

148 2.4 Material model

149 We used both linear on nonlinear viscoelasticity models to describe the time-dependent behaviour of
150 trabecular bone. The linear Kelvin-Voigt model or Prony series was employed to describe the time-
151 varying compliance, $D(t)$, given by

$$152 \quad D(t) = D_g + \sum_{i=1}^n D_i [1 - \exp(-t/\tau_i)] \quad (1)$$

153 where D_g is instantaneous compliance that describes the elastic response at time $t=0$, D_i are transient
154 retardation strengths associated with retardation times (τ_i). The nonlinear viscoelastic model was
155 based on the approach of Park and Schapery (1999) in which the time-varying compliance includes
156 nonlinear stress-dependent parameters, g_0 , g_1 , g_2 and α_σ , and is given by

$$157 \quad D(t) = g_0 D_g + g_1 g_2 \sum_{i=1}^n D_i [1 - \exp(-\frac{t}{\alpha_\sigma \tau_i})] \quad (2)$$

158 Following the approach used for untreated (or non-demineralised) bone (Manda et al. 2017), where
159 the unloading phase from the first cycle was assumed linear viscoelastic, the glassy or instantaneous
160 compliance (D_g), transient retardation strengths (D_i) and retardation times (τ_i) were evaluated by
161 minimising the errors between experimental measurements and Eq. 1. A three-term Prony series
162 ($n=3$) was chosen which gave a fitting error of less than 0.3%. The parameter g_0 is a nonlinear
163 instantaneous compliance parameter, the transient nonlinear parameter g_1 measures the effect of
164 nonlinearity in the transient compliance, g_2 describes the effect of loading rate on transient creep
165 response, and α_σ is a time-shift factor. Thereafter, the stress dependent nonlinear parameters g_2 and
166 α_σ in Eq. 2 were evaluated first by using the recovery strain response from cycles 2 to 8, followed by
167 evaluation of parameters of g_0 and g_1 using the entire unloading phase from each cycle (Manda et al.
168 2017). The nonlinear parameters obtained from each stress level were then expressed as smooth
169 second-order polynomial functions of stresses.

170 3 Results

171 Without exception, each sample exhibited classical rapid primary and slow secondary regimes of
172 creep behaviour across all stress levels. All 7 samples could be subjected to stress levels
173 corresponding to the highest designated strain level (3.5 %) without tertiary creep or failure.

174

175 3.1 Experimental observations

176 Figure 2b shows a strain response obtained from our tensile multiple-load-creep-unload-recovery
177 (MLCUR) experiment for one typical sample (medium porosity, BV/TV = 26.8 %). For this sample
178 the stress levels varied between 12.3 kPa and 106.9 kPa for the minimum and maximum applied
179 strain levels of 0.6 % and 3.5 %, respectively. The time-varying compliance, defined as the ratio
180 between time-varying strain and its corresponding stress level, was evaluated for both creep and
181 recovery phases, denoted as D_t^{cre} and D_t^{rec} respectively. Both time-varying compliances were found
182 to increase with time for all stress levels, as would be expected for a viscoelastic material (Fig. 2c
183 and 2d). For linear viscoelastic materials, the time-varying compliance curves would be identical for
184 all stress levels. However, the time-varying compliances, D_t^{cre} and D_t^{rec} , derived for demineralised
185 trabecular bone were found to vary with applied stress levels, indicating a nonlinear response.

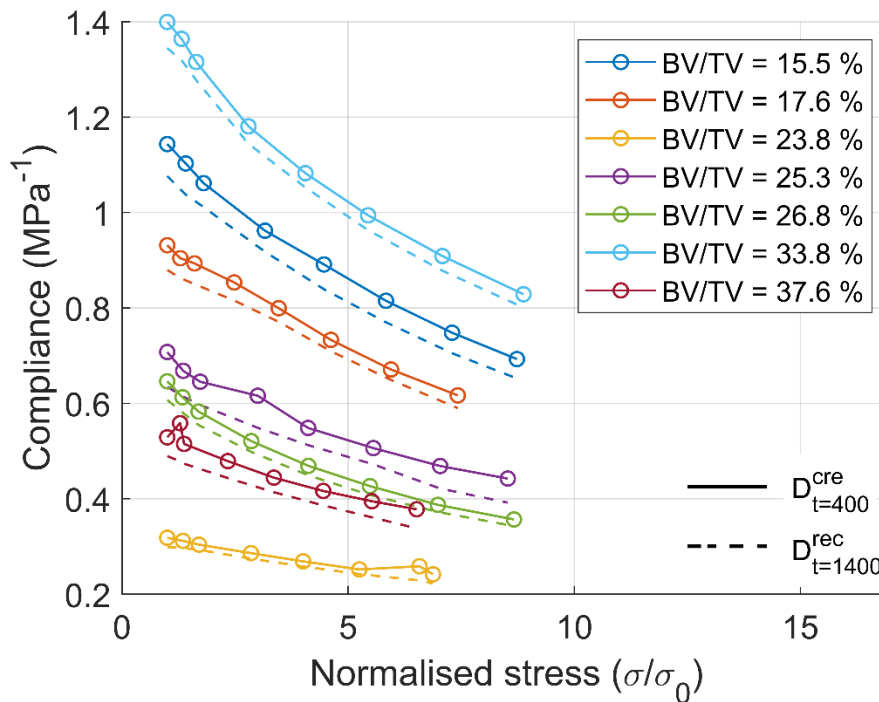
186 It was found that the time-varying compliance decreases with increasing stress levels (i.e. the curves
187 at lower stress levels are above those at the higher stress levels), and this is true for both creep and
188 recovery compliances (Fig 2c and 2d, respectively for the typical sample considered). This
189 decreasing trend was followed by all the samples tested, which demonstrates elastic stiffening with
190 increasing stress levels. It is also observed that the time-varying recovery compliance (D_t^{rec}) was
191 somewhat smaller than creep compliance (D_t^{cre}) in each corresponding cycle. It was apparent that the
192 creep compliance (D_t^{cre}) showed an increasing trend with time for all loading cycles, whereas the
193 recovery compliance (D_t^{rec}) reached a plateau after around 400 s of recovery. This indicates that
194 while irrecoverable strain develops in the loading and load holding phases, only viscoelastic strain is
195 recovered during unloading and recovery phases.

196 Compliance at the end of creep ($t = 400$ s) and recovery ($t = 1400$ s) from every loading cycle was
197 obtained (for example see Fig. 2c and 2d for the sample with BV/TV = 26.8%) and denoted as
198 $D_{t=400}^{cre}$ and $D_{t=1400}^{rec}$, respectively. This provided eight values of $D_{t=400}^{cre}$ and eight values $D_{t=1400}^{rec}$ for
199 every sample. Figure 3 shows both compliances plotted against normalised stress (σ/σ_o) defined as
200 the stress applied in each cycle divided by the stress applied in the first cycle (Manda et al. 2017) for
201 all the samples tested.

202 The creep compliance at $t = 400$ s ($D_{t=400}^{cre}$) was in the range of 0.24 to 1.40 MPa^{-1} . Recovery
203 compliance at $t = 1400$ ($D_{t=1400}^{rec}$) was in the range of 0.22 to 1.35 MPa^{-1} as shown in Fig. 3. The
204 decreasing trend in compliances with increased normalised stress level was observed for all tested

205 samples. These results also showed that the samples with higher BV/TV have, in general, lower
 206 compliance in comparison to samples with lower BV/TV. However, samples with BV/TV = 33.8 %
 207 and 23.8 % were found to be exceptions to this trend which cannot be readily explained. We believe
 208 that the micro-architectural orientation may have played a much stronger role for these two
 209 demineralised samples. For untreated (non-demineralised) bone it has been shown that bone mineral
 210 density (or indirectly BV/TV) which is the primary method to identify bone quality, does not often
 211 correlate with mechanical behaviour well (Schuit et al. 2004) and the porous microarchitecture of
 212 bone is an important determinant of its mechanical behaviour (Homminga et al. 2002). For the
 213 sample with BV/TV=23.8%, which has an extremely low compliance, it is also possible that during
 214 the experiment excessive cement was used which permeated through the sample. Therefore, we have
 215 excluded this sample from subsequent analysis.

216 Decreasing compliance with increased stress level indicates that the demineralised trabecular bone
 217 behaves in a nonlinear manner and it stiffens with increasing stress levels. Therefore, the use of a
 218 nonlinear constitutive model is required to describe the time-dependent behaviour of demineralised
 219 trabecular bone.

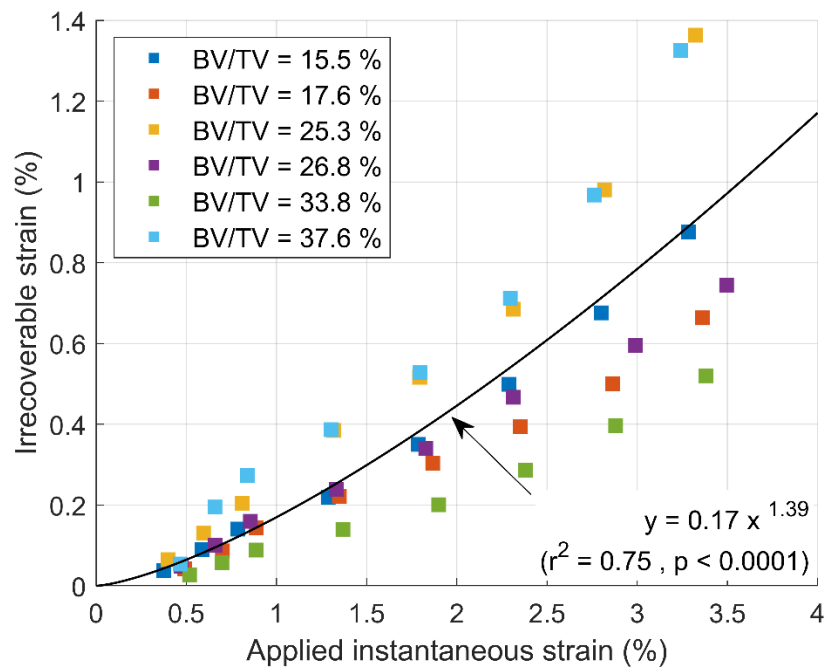


220

221 *Figure 3: Time-varying creep compliance at 400 s ($D_{t=400}^{cre}$) and recovery compliance at 1400 s ($D_{t=1400}^{rec}$)*
 222 *plotted against normalised stress for all 7 samples*

223 The compliances from the recovery regimes become constant (recovery curve reaches a plateau) in a
 224 short time, which indicates that the viscoelastic strain is perhaps completely recovered in the 1000 s
 225 recovery time provided in all cycles. The strains present at the end of each cycle were therefore
 226 deemed irrecoverable. This irrecoverable strain was found to exist even at the end of the first loading
 227 cycle corresponding to the smallest load level. Figure 4 shows the irrecoverable strain along with its
 228 applied static strain for all the cycles and all the samples. A power-law relationship ($r^2 = 0.75$, $p <$
 229 0.0001) was found between irrecoverable strain and applied static strain. However, no significant
 230 correlation was found between the irrecoverable strain and the original BV/TV (Fig. 4). It is clear
 231 that this irrecoverable strain increases with increasing applied load level for all demineralised
 232 trabecular bone samples.

233



234

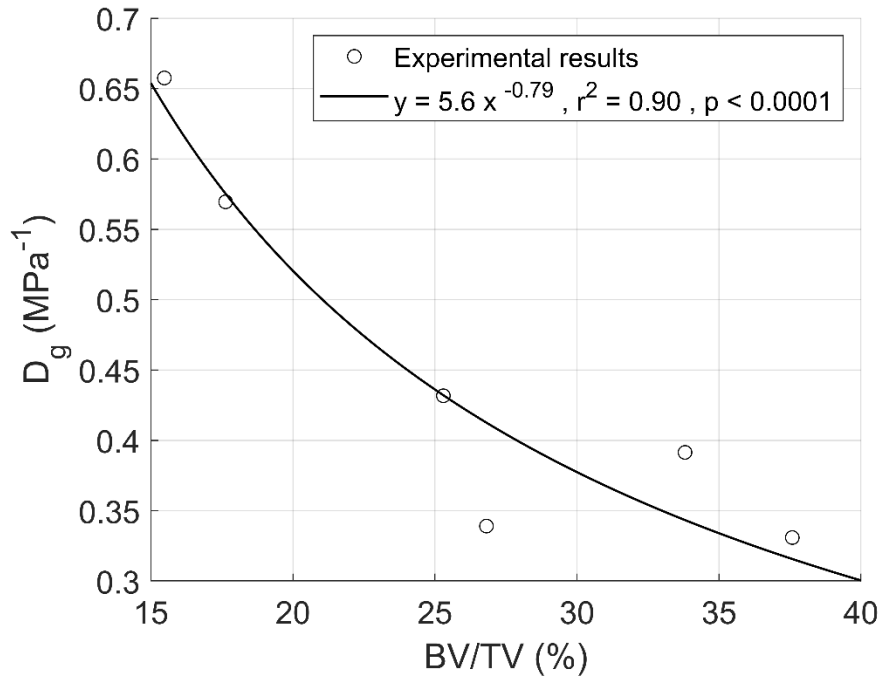
235 *Figure 4: Irrecoverable strain at the end of each loading cycle for all the samples plotted against the applied*
 236 *instantaneous strain (where plateau force was held constant during the test) with a power-law relationship*

237 3.2 Constitutive model

238 The instantaneous compliance (D_g) was found to be in the range of 0.33 to 0.66 MPa^{-1} (Fig. 5). It
 239 was also found that D_g decreases with increasing BV/TV with a power-law relationship (Fig. 5)

240

$$D_g = 7.4 \times (BV/TV)^{-0.91} \quad (r^2 = 0.90) \quad (3)$$

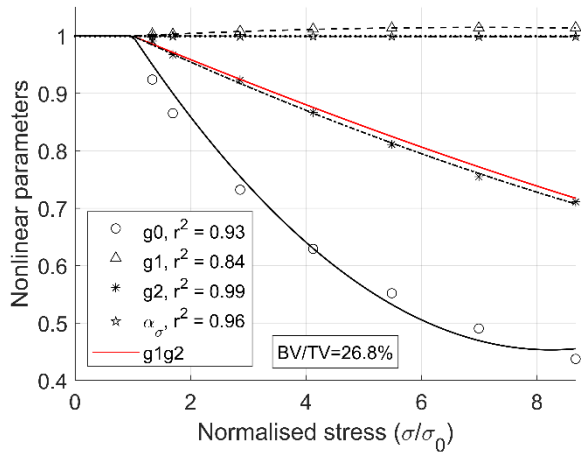


241

242 *Figure 5: Instantaneous compliance (D_g) plotted against BV/TV with a power law relationship.*

243 Figure 6a shows the variation for the typical sample considered (BV/TV = 26.8%), the values of g_0
 244 and g_2 decreased with increasing normalised stress (σ/σ_0), whereas the values of g_1 and α_σ were
 245 almost constant (Fig. 6a). The product of g_1g_2 , which affects the transient response was also found to
 246 decrease with increasing normalised stress. These observations led to the choice of a second-order
 247 polynomial function to represent the nonlinear viscoelastic parameters as functions of normalised
 248 stress, which produced coefficients of determination of $r^2 = 0.93, 0.84, 0.99$ and 0.96 for parameters
 249 g_0, g_1, g_2 and α_σ respectively (Fig. 6a). The decreasing trend of curves indicates that the
 250 demineralised trabecular bone stiffens with increased stress levels, and this elastic stiffening
 251 phenomenon was observed for all the samples tested. The nonlinear parameters for the 6 samples
 252 analysed are shown in Fig. 6b-6d and expressed as a second-order polynomial function with
 253 normalised stress. It can be seen that the variation described for the typical sample is largely followed
 254 by all. The decreasing trend of g_0 and g_1g_2 demonstrates that the demineralised trabecular bone
 255 sample experiences elastic stiffening in tension with increasing stress levels. The time-shift factor,
 256 α_σ , was found to remain almost constant for all samples.

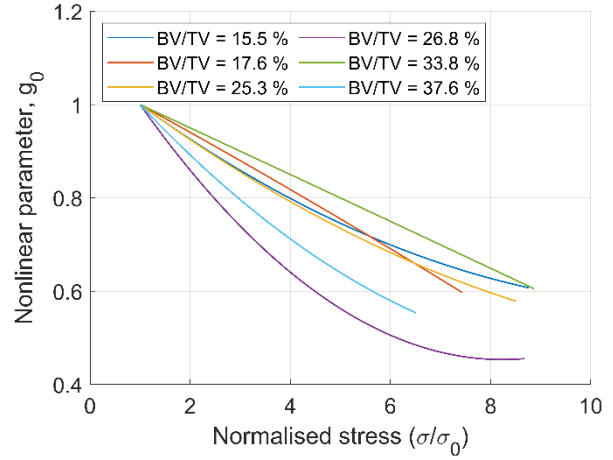
257



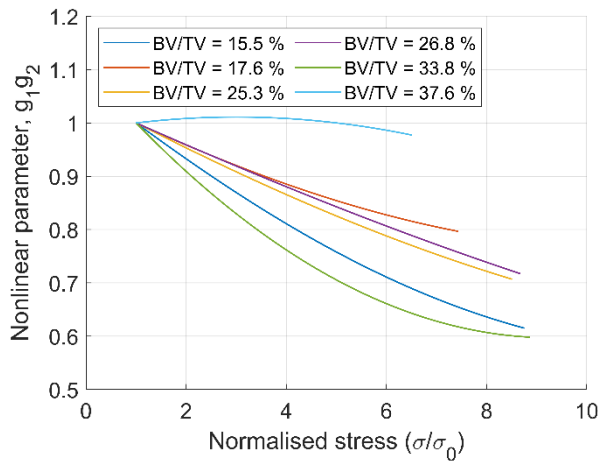
259

260

(a)



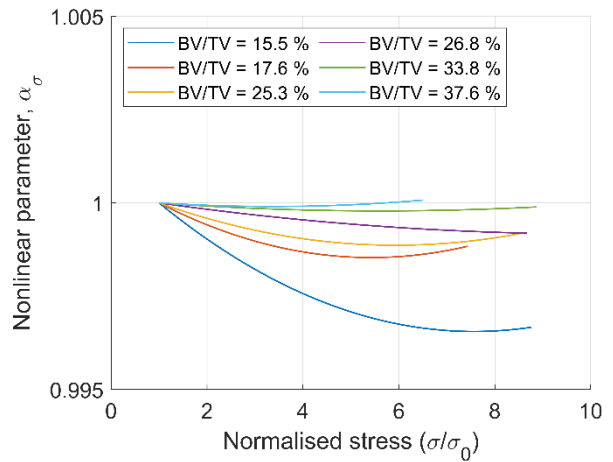
(b)



261

262

(c)

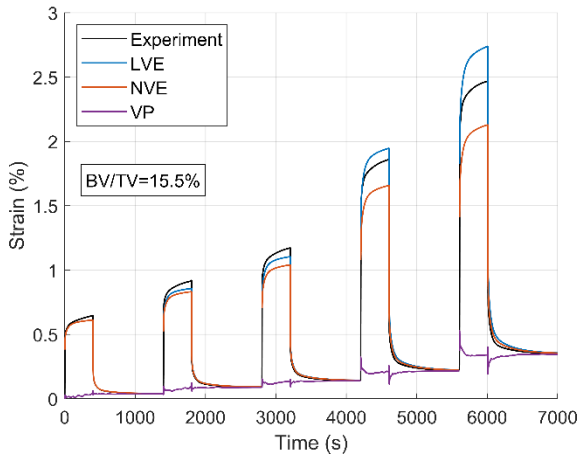


(d)

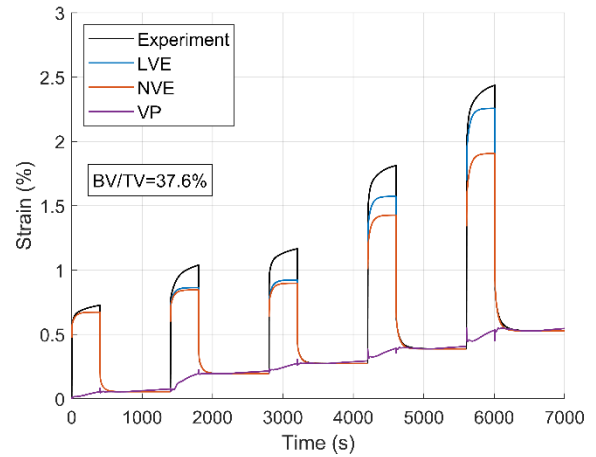
263 *Figure 6: Nonlinear viscoelastic parameters for the typical sample (a) and parameters for all 6 samples are*
 264 *expressed as second order polynomial functions of normalised stress: g_0 (b), g_1g_2 (c) and α_σ (d).*

265 The accuracy of linear viscoelastic (LVE) and nonlinear viscoelastic (NVE) constitutive models was
 266 compared with the experimental data. Figures 7a and b compare the experimentally obtained strain
 267 response to that obtained using LVE and NVE predictions for two representative samples with
 268 $BV/TV = 15.5\%$ and 37.6% . These samples had the lowest and highest BV/TV . For clarity, only the
 269 first 5 loading cycles are shown in Fig. 7. It can be seen that both models provide good predictions
 270 for the first loading cycle, however, at higher stress levels the NVE and LVE responses deviate from

271 the experimental curves. This is not unexpected as both LVE and NVE models are elastic models,
272 with NVE taking stress dependent nonlinearity into account. We have shown that the samples have
273 irrecoverable strains which elasticity models (linear or nonlinear) cannot incorporate. Figures 7a and
274 b also show irrecoverable strains (denoted as VP or viscoplastic). The viscoplastic (VP) strain was
275 evaluated by taking the difference between creep (which includes both viscoelastic and viscoplastic
276 strains) and recovery curves (viscoelastic strains only). In Fig. 7c and d, the irrecoverable portion of
277 the strain was removed from the experimental curve and it was then plotted against predictions of the
278 LVE and NVE models. It is clear that the NVE constitutive model provides a more accurate
279 prediction of the viscoelastic behaviour of demineralised bone, whereas the LVE constitutive model
280 only gives a reasonable prediction at low loading cycles. The LVE model over-predicts the strain
281 response at the higher stress levels, which also indicates that the demineralised trabecular bone
282 undergoes elastic stiffening at higher stress levels.



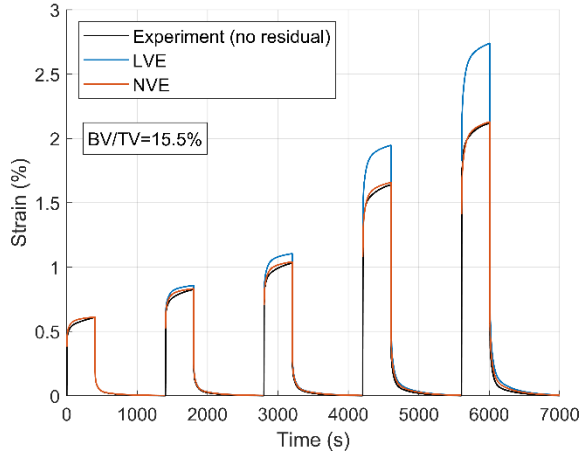
283



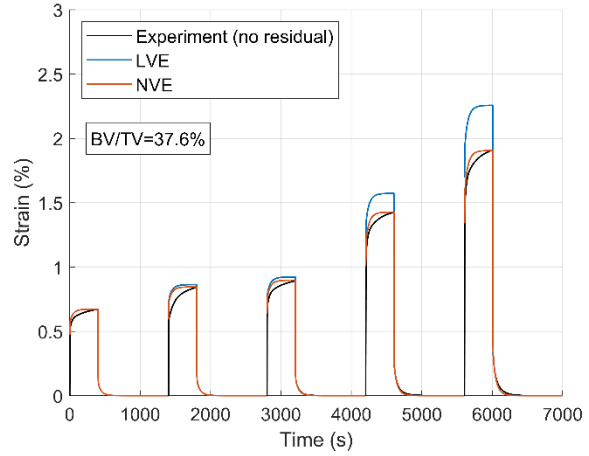
284

(a)

(b)



285



286

(c)

(d)

287 *Figure 7: The comparison of experimental strain response and constitutive model predictions. Experimental*
 288 *response and the predicted LVE, NVE strain response and viscoplastic strain (a & b), experimental strain*
 289 *response (with residual strain excluded) compared with predicted linear and nonlinear viscoelastic strain*
 290 *response (c & d), for two samples with lowest and highest BV/TV considered.*

291

292 4 Discussion

293 As stated in the introduction, untreated (non-demineralised) trabecular bone has been studied
 294 extensively for its time-independent properties and there have also been a number of studies to
 295 investigate its time-dependent behaviour through creep, relaxation and dynamic loading.

296 Demineralised bone has been primarily examined for its time-independent properties and studies on
297 its time-dependent behaviour have been extremely limited.

298 Tensile multiple-load-creep-unload-recovery (MLCUR) experiments on demineralised trabecular
299 bone undertaken in this study show that its response to mechanical forces is time-dependent and the
300 strain includes recoverable and irrecoverable components, even at low-stress levels. The results also
301 show that this time-dependent behaviour of demineralised trabecular bone varies nonlinearly with the
302 applied stress. The nonlinear viscoelastic model can predict demineralised trabecular bone's time-
303 dependent behaviour well if the irrecoverable strain is excluded. As found in previous time-
304 independent monotonic loading studies our results also show that demineralised trabecular bone
305 stiffens at increased stress levels.

306 The MLCUR experiments have been previously used to investigate untreated trabecular bone's time-
307 dependent behaviour in compression (Manda et al. 2016, 2017; Xie et al. 2017). This study employed
308 a similar approach to evaluate the time-dependent behaviour of demineralised trabecular bone in
309 tension. We assumed that the first strain level of 0.6% to be in the linear elastic range. Bowman et al
310 (1996) showed that demineralised bone does not yield up to an apparent strain of 10% in tension
311 (Bowman et al. 1996) and that creep failure strains are in the range 8.8-21.1% (Bowman et al. 1999).
312 In fact, Bowman et al. (1999) applied preconditioning cycles between 0-5% strain before applying a
313 loading ramp to obtain linear region of the stress-strain curve. Predictions made using the LVE model
314 indicate that this assumption is accurate for slightly higher strains as well (e.g. see second load cycle
315 in Fig. 7).

316 The observed creep compliances for demineralised trabecular bone in tension were in the range 0.22
317 to 1.40 MPa^{-1} while the creep compliance in compression for untreated bone have been found to be in
318 the range 1.08×10^{-3} to $4.17 \times 10^{-3} \text{ MPa}^{-1}$ (Manda et al. 2016). As expected, this indicates that the
319 demineralised trabecular bone is much more flexible than untreated bone. From our experiments the
320 long-term modulus of demineralised bone was calculated by taking reciprocal of the instantaneous
321 compliance (D_g). The evaluated modulus was found to be of similar order as in previous studies for
322 demineralised cortical bone (Burstein et al. 1975; Bowman et al. 1996; Catanese et al. 1999;
323 Novitskaya et al. 2011) and demineralised trabecular bone (Chen et al. 2011; Xie et al. 2018b).
324 However, above-cited studies were all limited to monotonic or cyclic loading.

325 Bone is recognised as time-dependent material in which the strain (or stress) response to a force (or
326 displacement) is not instantaneous. Similar to untreated trabecular bone (Manda et al. 2017; Xie et al.
327 2017), demineralised trabecular bone's time-dependent behaviour is nonlinearly related to the applied
328 stress level. Our MLCUR experiments show that at higher stress levels the strain response is smaller
329 than what would be expected if a linear viscoelastic model were used. This indicates that
330 demineralised bone stiffens at higher stress levels. This result is in agreement with previous
331 monotonic loading studies in which the well-known J-shaped stress-strain curve has been observed,
332 not only for demineralised bone (Bowman et al. 1996; Xie et al. 2018b) and actin networks
333 (Schmoller et al. 2010) but also for untreated bone (Kim et al. 2011; Xie et al. 2017). The explanation
334 for the J curve is that initially the kinks in the collagen are straightened out then the collagen fibres
335 start carrying the loads.

336 Bone volume ratio (BV/TV) or porosity of the bone has been used extensively and successfully to
337 describe bone's time-independent properties (Carter and Hayes 1977; Currey 1988; Gibson and
338 Ashby 1999; Gibson 2005). Some previous study have also used BV/TV in the study of bone's time-
339 dependent behaviour (Manda et al. 2016; Xie et al. 2017). This study shows that time-dependent
340 response of demineralised bone is also strongly associated with BV/TV of the samples prior to
341 demineralisation. Both creep and recovery compliance values largely follow the BV/TV trends (see
342 Fig. 3). As would be expected, samples with higher BV/TV generally have lower compliance.

343 Our experiments show that unloading results in some irreversible strains at the end of each loading
344 cycle, which increases with increasing stress levels. However, we did not find an apparent
345 relationship between irrecoverable strain and BV/TV. The post-elastic mechanical behaviour is likely
346 to be much more strongly linked to micro-architecture than simply BV/TV of the samples. Reasons
347 for apparent plastic behaviour of bone and demineralised bone have been discussed in previous
348 studies. By conducting uniaxial nano-mechanical compression on cylindrical samples Tertuliano and
349 Greer (2016) proposed that inter-fibrillar sliding through shear of extra-fibrillar matrix was the
350 mechanism of plasticity in bone, which was also suggested by Gupta et al. (2005, 2006). This
351 irrecoverable strain could also be due to inter-fibrillar sliding at nano-scale. This irrecoverable
352 deformation in collagen needs to be emphasised, as it is generally ignored in two-phase composite
353 models of bone (Lubarda et al. 2012).

354 Composite models of bone can help illustrate the complex interrelationship between bone
355 microstructure and material properties of constituents. In particular, bone is frequently modelled as a

356 two-phase composite, hydroxyapatite mineral crystals dispersed in an organic matrix. This study
357 shows that the time-dependent behaviour of bone's organic phase can be described using a nonlinear
358 viscoelastic model, which provides a good prediction for recoverable (elastic) strain response at
359 varying load levels. These developed models can be used in conjunction with the mechanical
360 properties of bone's mineral phase for evaluating the influence of the two phases on the time-
361 dependent mechanical response.

362 This study suffers from a number of limitations. Firstly, all the tests were conducted at room
363 temperature; creep behaviour has been reported to be temperature-dependent for bone (Bonfield and
364 Li 1968; Bowman et al. 1998), so it is likely that the demineralised trabecular bone's viscoelastic
365 behaviour is also temperature-dependent. Secondly, it is not possible in practice to perform ideal
366 creep-recovery experiments and in the tests conducted, the time interval to loading and unloading is
367 finite (e.g. 1 s to reach 1% strain with our designated strain rate 0.01 s^{-1}). Small viscoelastic
368 deformations are likely to occur during loading and unloading.

369 In conclusion, this study shows that the response of demineralised trabecular bone samples to
370 mechanical forces is time-dependent and it is nonlinearly related to its applied stress levels – it
371 stiffens with increased stress level. Some irrecoverable strain exists even at load cycles
372 corresponding to small strains. Irrecoverable strain, however, is not related to a sample's pre-
373 demineralised BV/TV. The developed nonlinear time-dependent constitutive model can be
374 incorporated together with properties of the mineral phase to generate a composite model of bone.

375 **5 Conflict of Interest**

376 The authors declare that the research was conducted in the absence of any commercial or financial
377 relationships that could be construed as a potential conflict of interest.

378 **6 Author Contributions**

379 S. Xie: Designed study, conducted experiment, analysed data and drafted manuscript

380 R. Wallace: Designed study, conducted experiment and revised manuscript critically

381 P. Pankaj: Designed study, analysed data and revised manuscript critically

382 **7 Funding**

383 We gratefully acknowledge the financial support of EPSRC [Grant EP/K036939/1].

384 **8 Acknowledgments**

385 We thank Dr Anthony Callanan from The University of Edinburgh for his support in conducting the
386 mechanical tests.

387

388 **References**

- 389 Bonfield W, Li CH (1967) Anisotropy of nonelastic flow in bone. *J Appl Phys* 38:2450–2455.
390 <https://doi.org/10.1063/1.1709926>
- 391 Bonfield W, Li CH (1968) The temperature dependence of the deformation of bone. *J Biomech*
392 1:323–329. [https://doi.org/10.1016/0021-9290\(68\)90026-2](https://doi.org/10.1016/0021-9290(68)90026-2)
- 393 Bowman SM, Gibson LJ, Hayes WC, McMahon TA (1999) Results from demineralized bone creep
394 tests suggest that collagen is responsible for the creep behavior of bone. *J Biomech Eng*
395 121:253–258. <https://doi.org/10.1115/1.2835112>
- 396 Bowman SM, Guo XE, Cheng DW, et al (1998) Creep contributes to the fatigue behavior of bovine
397 trabecular bone. *J Biomech Eng* 120:647–654
- 398 Bowman SM, Keaveny TM, Gibson LJ, et al (1994) Compressive creep behavior of bovine
399 trabecular bone. *J Biomech* 27:301–310
- 400 Bowman SM, Zeind J, Gibson LJ, et al (1996) The tensile behavior of demineralized bovine cortical
401 bone. *J Biomech* 29:1497–1501. [https://doi.org/10.1016/0021-9290\(96\)84546-5](https://doi.org/10.1016/0021-9290(96)84546-5)
- 402 Burstein AH, Zika JM, Heiple KG, Klein L (1975) Contribution of collagen and mineral to the
403 elastic-plastic properties of bone. *J Bone Joint Surg Am* 57:956–961
- 404 Carter DR, Hayes WC (1977) The compressive behavior of bone as a two-phase porous structure. *J*
405 *Bone Jt Surg*, 59:954-962. <https://doi.org/10.2106/00004623-197759070-00021>
- 406 Castro-Ceseña AB, Sánchez-Saavedra MP, Novitskaya EE, et al (2013) Kinetic characterization of
407 the deproteinization of trabecular and cortical bovine femur bones. *Mater Sci Eng C* 33:4958–
408 4964. <https://doi.org/10.1016/j.msec.2013.08.022>
- 409 Catanese J, Iverson EP, Ng RK, Keaveny TM (1999) Heterogeneity of the mechanical properties of
410 demineralized bone. *J Biomech* 32:1365–1369. [https://doi.org/10.1016/S0021-9290\(99\)00128-1](https://doi.org/10.1016/S0021-9290(99)00128-1)
- 411 Chen PY, McKittrick J (2011) Compressive mechanical properties of demineralized and
412 deproteinized cancellous bone. *J Mech Behav Biomed Mater* 4:961–973.
413 <https://doi.org/10.1016/j.jmbbm.2011.02.006>

- 414 Chen PY, Toroian D, Price PA, McKittrick J (2011) Minerals form a continuum phase in mature
415 cancellous bone. *Calcif Tissue Int* 88:351–361. <https://doi.org/10.1007/s00223-011-9462-8>
- 416 Currey JD (1969) The relationship between the stiffness and the mineral content of bone. *J Biomech*
417 2:477–480. [https://doi.org/10.1016/0021-9290\(69\)90023-2](https://doi.org/10.1016/0021-9290(69)90023-2)
- 418 Currey JD (1988) The effect of porosity and mineral content on the Young's modulus of elasticity of
419 compact bone. *J Biomech* 21:131–139. [https://doi.org/10.1016/0021-9290\(88\)90006-1](https://doi.org/10.1016/0021-9290(88)90006-1)
- 420 Currey JD (1964) Three analogies to explain the mechanical properties of bone. *Biorheology* 2:1–10
- 421 Gibson LJ (2005) Biomechanics of cellular solids. *J Biomech* 38:377–399.
422 <https://doi.org/10.1016/j.jbiomech.2004.09.027>
- 423 Gibson LJ, Ashby MF (1999) Cellular solids: structure and properties. Cambridge university press
- 424 Gupta HS, Seto J, Wagermaier W, et al (2006) Cooperative deformation of mineral and collagen in
425 bone at the nanoscale. *Proc Natl Acad Sci* 103:17741–17746.
426 <https://doi.org/10.1073/pnas.0604237103>
- 427 Gupta HS, Wagermaier W, Zickler GA, et al (2005) Nanoscale deformation mechanisms in bone.
428 *Nano Lett* 5:2108–2111. <https://doi.org/10.1021/nl051584b>
- 429 Homminga J, McCreadie BR, Ciarelli TE, et al (2002) Cancellous bone mechanical properties from
430 normals and patients with hip fractures differ on the structure level, not on the bone hard tissue
431 level. *Bone* 30:759–764. [https://doi.org/10.1016/S8756-3282\(02\)00693-2](https://doi.org/10.1016/S8756-3282(02)00693-2)
- 432 Katz JL (1980) Anisotropy of Young's modulus of bone. *Nature* 283:106–107
- 433 Keaveny TM, Pinilla TP, Crawford RP, et al (1997) Systematic and random errors in compression
434 testing of trabecular bone. *J Orthop Res* 15:101–110. <https://doi.org/10.1002/jor.1100150115>
- 435 Kim D-G, Shertok D, Ching Tee B, Yeni YN (2011) Variability of tissue mineral density can
436 determine physiological creep of human vertebral cancellous bone. *J Biomech* 44:1660–1665.
437 <https://doi.org/10.1016/j.jbiomech.2011.03.025>
- 438 Levrero-Florencio F, Margetts L, Sales E, et al (2016) Evaluating the macroscopic yield behaviour of
439 trabecular bone using a nonlinear homogenisation approach. *J Mech Behav Biomed Mater*

440 61:384–396

441 Lievers WB, Lee V, Arsenault SM, et al (2007) Specimen size effect in the volumetric shrinkage of
442 cancellous bone measured at two levels of dehydration. *J Biomech* 40:1903–1909.
443 <https://doi.org/10.1016/j.jbiomech.2006.09.002>

444 Lubarda VA, Novitskaya EE, McKittrick J, et al (2012) Elastic properties of cancellous bone in terms
445 of elastic properties of its mineral and protein phases with application to their osteoporotic
446 degradation. *Mech Mater* 44:139–150. <https://doi.org/10.1016/j.mechmat.2011.06.005>

447 Manda K, Wallace RJ, Xie S, et al (2017) Nonlinear viscoelastic characterization of bovine
448 trabecular bone. *Biomech Model Mechanobiol* 1:173–189

449 Manda K, Xie S, Wallace RJ, et al (2016) Linear viscoelasticity - bone volume fraction relationships
450 of bovine trabecular bone. *Biomech Model Mechanobiol* 15:1631–1640

451 Novitskaya E, Chen PY, Lee S, et al (2011) Anisotropy in the compressive mechanical properties of
452 bovine cortical bone and the mineral and protein constituents. *Acta Biomater* 7:3170–3177.
453 <https://doi.org/10.1016/j.actbio.2011.04.025>

454 Novitskaya E, Lee S, Lubarda VA, McKittrick J (2013) Initial anisotropy in demineralized bovine
455 cortical bone in compressive cyclic loading-unloading. *Mater Sci Eng C* 33:817–823.
456 <https://doi.org/10.1016/j.msec.2012.11.006>

457 Park SW, Schapery RA (1999) Methods of interconversion between linear viscoelastic material
458 functions. Part I - a numerical method based on Prony series. *Int J Solids Struct* 36:1653–1675.
459 [https://doi.org/10.1016/S0020-7683\(98\)00055-9](https://doi.org/10.1016/S0020-7683(98)00055-9)

460 Schmoller KM, Fernández P, Arevalo RC, et al (2010) Cyclic hardening in bundled actin networks.
461 *Nat Commun* 1:134. <https://doi.org/10.1038/ncomms1134>

462 Schuit SCE, Van Der Klift M, Weel AEAM, et al (2004) Fracture incidence and association with
463 bone mineral density in elderly men and women: The Rotterdam Study. *Bone* 34:195–202.
464 <https://doi.org/10.1016/j.bone.2003.10.001>

465 Sharp DJ, Tanner KE, Bonfield W (1990) Measurement of the density of trabecular bone. *J Biomech*
466 23:853–857. [https://doi.org/10.1016/0021-9290\(90\)90032-X](https://doi.org/10.1016/0021-9290(90)90032-X)

- 467 Tertuliano OA, Greer JR (2016) The nanocomposite nature of bone drives its strength and damage
468 resistance. *Nat Mater* 15:1195–1202. <https://doi.org/10.1038/nmat4719>
- 469 Vahey JW, Lewis JL, Vanderby R (1987) Elastic moduli, yield stress, and ultimate stress of
470 cancellous bone in the canine proximal femur. *J Biomech* 20:29–33.
471 [https://doi.org/10.1016/0021-9290\(87\)90264-8](https://doi.org/10.1016/0021-9290(87)90264-8)
- 472 Wallace RJ, Pankaj P, Simpson AHRW (2013) The effect of strain rate on the failure stress and
473 toughness of bone of different mineral densities. *J Biomech* 46:2283–2287.
474 <https://doi.org/10.1016/j.jbiomech.2013.06.010>
- 475 Xie S., Wallace RJ, Pankaj P (2018a) Characterisation of mechanical behaviour of demineralised and
476 deproteinised trabecular bone samples [<https://doi.org/10.7488/ds/2339>]. The University of
477 Edinburgh
- 478 Xie S, Manda K, Wallace RJ, et al (2017) Time Dependent Behaviour of Trabecular Bone at Multiple
479 Load Levels. *Ann Biomed Eng* 45:1219–1226
- 480 Xie S, Wallace RJ, Callanan A, Pankaj P (2018b) From Tension to Compression: Asymmetric
481 Mechanical Behaviour of Trabecular Bone’s Organic Phase. *Ann Biomed Eng* 46:801–809
- 482
- 483
- 484
- 485

486 **Supplementary information**

487

488 Constitutive model:

489

490 The nonlinear viscoelastic model was based on Manda et al. (2017) which used the
491 Schapery's nonlinear viscoelastic constitutive law (Shapery 1969). In this the strain
492 response to a suddenly applied stress is given by

493

494
$$\varepsilon(t) = g_0 D_g \sigma + g_1 \int_0^t \Delta D (\psi^t - \psi^\tau) \frac{d(g_2 \sigma)}{d\tau} d\tau \quad (1)$$

495

496
$$\psi^t = \int_0^t \frac{d\tau'}{\alpha_{\sigma(\tau')} \alpha_{T(\tau')} \alpha_{e(\tau')}} \quad (2)$$

497

498 where D_g is instantaneous compliance, g_0 , g_1 , g_2 and α_σ are stress-dependent nonlinear
499 viscoelastic parameters, σ is applied stress and ψ^t is reduced time. Parameters α_σ , α_T
500 and α_e are stress, temperature and other environment time-shift factors, respectively. The
501 effects of temperature (α_T) and other environment variables (α_e) are not considered;
502 consequently, these two parameters are unity. The transient compliance, ΔD , in equation
503 (1) is represented by Prony series as

504

505
$$\Delta D(\psi^t) = \sum_1^n D_n [1 - \exp(-\psi^t / \tau_n)] \quad (3)$$

506

507 where D_n is n th coefficient of the Prony series associated with n th retardation time, τ_n .

508 Therefore, the nonlinear time-dependent compliance can be rewritten as

509
$$D(t) = g_0 D_g + g_1 g_2 \sum_1^n D_n [1 - \exp(-\frac{t}{\alpha_\sigma \tau_n})]$$
 (1)

510 This equation reduces to linear viscoelasticity equation if all the stress-dependent
511 nonlinear parameters are unity.

512

513 Parameters fitting:

514 We assume that the first cycle (lowest strain) is linear viscoelastic. Therefore, D_g , D_n and
515 τ_n were evaluated by minimising the errors between experimental measurement and the
516 linear viscoelastic equation. Three Prony terms ($n=3$) were chosen after a number of
517 fittings and we found that this gave fitting error of less than 0.3%.

518 The nonlinear parameters, g_2 and α_σ were first evaluated by using the recovery part of the
519 experimental curve. Then the the nonlinear parameters g_0 and g_1 were evaluated by using
520 the entire unloading phase from each cycle. The evaluated nonlinear parameters obtained
521 from each stress level were then expressed as smooth second-order polynomial functions
522 of stresses.

523

524 **References:**

- 525 1. Manda K, Wallace RJ, Xie S, Levrero-Florencio F, Pankaj P. Nonlinear viscoelastic
526 characterization of bovine trabecular bone. *Biomech Model Mechanobiol.* 2017;16:173–89.
- 527 2. Schapery RA. On the characterization of nonlinear viscoelastic materials. *Polym Eng Sci.*
528 1969;9(4):295–310.

529

530